Y@Pt/C Core-Shell Electro-Catalyst for Oxygen Reduction Reaction

M.M. Tellez-Cruz[1], J.F. Godínez-Salomón[1], O. Solorza-Feria[1].*

[1]Departamento de Química, Centro de Investigación y Estudios Avanzados del IPN, Av. IPN 2508, Col. San Pedro Zacatenco, A. Postal 14-740, 07360 México D.F., México.
*Tel: 011 +52 +55 5747-3715 ; e-mail: osolorza@cinvestav.mx

ABSTRACT

The synthesis of yttrium decorated platinum core-shell nanocatalyst for the oxygen reduction reaction (ORR) in acid media is presented. The core of the nanocatalysts was prepared through colloidal reduction of YCl_3 with $NaBH_4$ while the shell was deposited by galvanic displacement on the surface of Y nanoparticles. The presence of Pt in the core was proved by XRD. TEM micrographs have showed highly dispersed nanoparticles with an average 2 nm. The presence of Y and Pt on 81 and 19 wt. % respectively was confirmed by EDAX. The electrochemical performance of Y@Pt/C is evaluated by cyclic voltammetry, CO stripping and using rotating disk electrode setup, was carried out for the ORR in HClO4 electrolyte; indicated that have more catalytic activity than that of commercial 20% Pt / C-Etek® catalyst, used as reference.

Keywords: Y@Pt / C; ORR; core-shell.

1. Introduction

Fuel cells offer a potentially cleaner and more efficient source of energy due to their high efficiency and low emissions compared with internal combustion engines and other energy-conversion devices. However, two major technical gaps limit their commercialization: cost and reliability. Currently, platinum (Pt)-based catalysts and their corresponding cathode catalyst layers are among the major causes of limited performance and high cost for proton exchange membrane fuel cells (PEMFC), although these are the most promising and practical fuel cell catalysts [1].

In a PEM fuel cell, the major limit on performance is the cathodic oxygen reduction reaction (ORR). The cathode of the fuel cell is the electrode where oxygen is reduced to water by the following reaction, known as the oxygen reduction reaction (ORR):

$$O_2 + 4H^+ + 4e^- \rightarrow 2H_2O \text{ (1.23 V vs. NHE [2])} \quad (1)$$

This reaction is slow, for that reason Pt is used as a catalyst, and requires a large overpotential before reaction kinetics increase. Consequently, developing alternative catalysts to Pt for the ORR in PEMFC is a major goal for researchers and a necessity for the commercialization of fuel cells.

Numerous efforts have been devoted to the optimization of the existing platinum nanoparticle catalysts and to the design of new catalysts with less Pt. In addition to nanoparticles morphology control, recent research has also focused on fabrication of multicomponent metal catalysts to modify the Pt electronic structure affected by the second transition metal with the improvement in the catalytic activity for the ORR [3]. Some studies have shown good catalytic activity for the ORR in metals and alloys in compared with Pt [4] [5] [6] [7]. For this reason in this work was decided to synthesize a core-shell Y@Pt catalyst in 80:20 wt. % Y: Pt for the ORR.

2. Experimental

2.1 Catalyst synthesis

Vulcan carbon was heat treated at 500 ° C for 2h under N_2. Subsequently 300 mg of it is heat treated carbon added 50 mL of 50% HNO_3 and sonicated for 1 h, over this were refluxed for 1h. It was dried at 120° C for 1 h in N_2 atmosphere. The acid treated carbon was dispersed in 50 mL of water and added ethanolamine in 1:1 molar ratio was allowed 1h to reflux. It was dried at 120 ° C for 1 h in N_2 atmosphere.

Yttrium nanoparticles were synthesized by the borohydride reduction method in ethanol. 200 mg of treated carbon were mixed with YCl_3 (nominal weight C:Y ratio 70:30), and in 1:1 molar ratio TBAB:YCl_3 in 70 mL of ethanol. The mixture was sonicated 10 min and magnetically stirred during 20 min in a N_2 atmosphere.

Then, $NaBH_4$ (in the molar ratio 3.3:1 $NaBH_4$:Y) dissolved in 20 mL of ethanol was added drop by drop to promote the reduction, and was left 1 hour, then are added 10 mL of H_2O.

2 mL of K_2PtCl_6 (nominal weight Y:Pt ratio 80:20) dissolved in 30 mL of water was added, and subsequently the temperature is increased to boiling. Once at reflux is added drop by drop the remaining solution. He left in 4h reaction. Was separated by centrifugation and washings were performed with water. Finally dried at 150 ° C for 2 hours in CO atm.

2.2 Electrochemical measurement

The electrochemical measurements were conducted at 25°C in a typical three electrodes cell filled with 0.1 M $HClO_4$ electrolyte solution. Disk potential was controlled with a potenciostato /galvanostat (PARSTAT model 2273). A Pt mesh was used as counter-electrode and the potentials were determined using a freshly prepared reversible hydrogen electrode (RHE).

Catalyst inks were prepared as follows: 12 mg of the corresponding Y@Pt/C catalyst (2 nm) and 2mL of solution of 20% isopropanol and 0.02% Nafion ionomer (5 % wt.) were dispersed ultrasonically. 10 µL of the catalyst ink was added onto a polished glassy carbon electrode and the film was dried by air flow at 45°C leading to a Pt loading of 18 $\mu g_{Pt}\ cm^{-2}$. The CV curves of these catalysts were recorded in deaerated electrolyte solution at a sweep rate of 50 mV s^{-1} between 0.05 V and 1.2 V until a stable voltammogram was recorded (around 30 cycles).

The ORR polarization curves for the RDE in an O_2-saturated 0.1 M $HClO_4$ solution at 25°C were obtained at a sweep rate of 20 mV s^{-1} through a positive sweep at rotation rates of 400, 900, 1600 and 2500 rpm. Additionally, the CO-stripping charge was used to determine the electrochemical surface area (ECSA). For CO stripping measurements, the catalyst surface was previously saturated with CO by bubbling CO through the electrolyte solution polarizing the electrode at 0.1 V/RHE for 5 min. Then the remaining CO was purged by flowing N_2 for 10 min before measurements which were performed at scan rate of $20mVs^{-1}$.

2.3 X-ray diffraction (XDR)

Crystal structure identification was performed by X-ray diffraction (XRD) using a diffractometer (PAN-analytical R&D Empyrean) whit monochromatic Cu-Kα radiation (λ= 1.5405 Å) in a 2θ range from 5° to 90°.

2.4 High resolution transmission electron microscopy (HRTEM)

Particle size, morphology and distribution of the Y@Pt nanomaterial were assessed from high resolution transmission electron microscopy (HRTEM) from JEM ARM200F instrument operated at an accelerated voltage of 300 kV. Y@Pt nanoparticle size distribution was calculated based on random counting of particles from TEM with image J software.

2.5 Scanning electron microscopy (SEM) and energy dispersive X-ray analysis (EDX)

Secondary electron images and the elemental mapping of the Y@Pt catalysts were determined by the EDX technique coupled to a scanning electron microscopy by AURIGA-39-16 applying 10 kV.

3. Results and discussion

3.1 X-ray diffraction (XDR)

The Fig. 1 shows XRD pattern for Y@Pt after removing the background. The results reveal that there are defined peaks characteristic diffraction inorganic sample plus they are wide, which allows qualitatively interpret that is materials of small crystallite sizes. This pattern show metallic Pt phase, besides Pt_3Y phase which has a positive displacement of the diffraction angles which is qualitatively rationalize with a tension process caused by the compression of the lattice crystal of Pt in Pt_3Y phase because platinum attempts to adopt the Y structure during the galvanic replacement [8]. A compact Pt surface layer with moderate lattice contraction seemingly is a common structural feature that enhances the ORR activity [9]. Additionally the phase of pure yttrium is not shown because it is at the center of the particle, which is covered with platinum.

The presence of a maximum width at low diffraction angles (24-26 °) associated with the carbon used as support was observed. Finally the quantitative phase analysis reveals the presence of Pt and C in the relative weight fraction of 2.3 and 97.7 wt. %

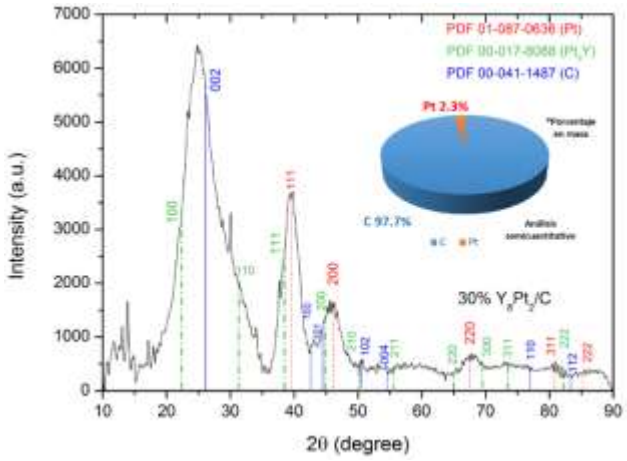

Fig. 1 XRD two theta scan after background subtractions for samples Y@Pt/C

3.2 High resolution transmission electron microscopy (HRTEM)

Fig. 2 shows representative images of low and high magnification transmission micrographs for Y@Pt/C, showed nanoparticles with cubeoctahedron like shape, well distributed and rather uniform on carbon. The histogram for particle size distribution, includes analysis of several different regions of the catalysts, revealed that the average particle size is ca. 2 nm with a very small size distribution with particles from 1-5 nm. Additionally you can see the lattice of particle in uniform form.

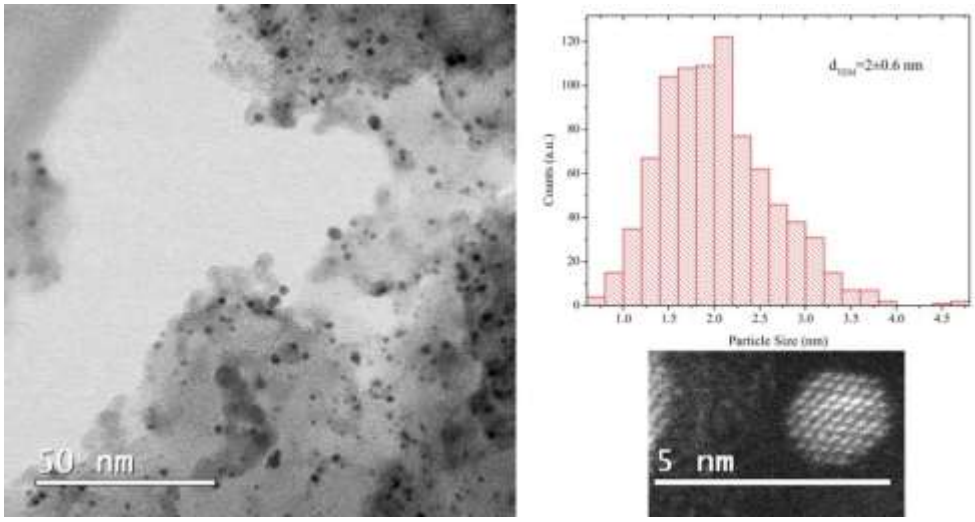

Fig. 2 High resolution TEM image of Y@Pt/C nanocatalyst.

3.3 Scanning electron microscopy (SEM) and energy dispersive X-ray analysis (EDX)

Fig. 3 shows images of the elemental EDX mapping on the sample, the results suggested a uniform Y and Pt elemental phase distribution. Note that these percentages are close to the theoretically estimated during synthesis of materials.

3.4 Electrochemical measurement

The catalysts were electrochemically characterized by cyclic voltammetry (CV). Figure 4A shows the cyclic voltammograms of Y@Pt/C. The curves showed three different potential regions. The hydrogen underpotential deposition domain (Hupd) were well defined, between 0.05 and 0.35 V. The voltammetry curves for the Y@Pt catalyst did not revealed anodic current associated to oxidation/dissolution of Y, demonstrating that the core of Y is completely covered by the Pt Shell.

The potential range between 0.4 V and ~ 0.75 V correspond to "double layer" region. The presented width peak here observed was attributed to the quinone/hydro-quinone equilibrium owing to the carbon support [10]. Above 0.8 V corresponding to OH adsorption area, during the positive sweep and then subsequent reduction in back sweep took place.

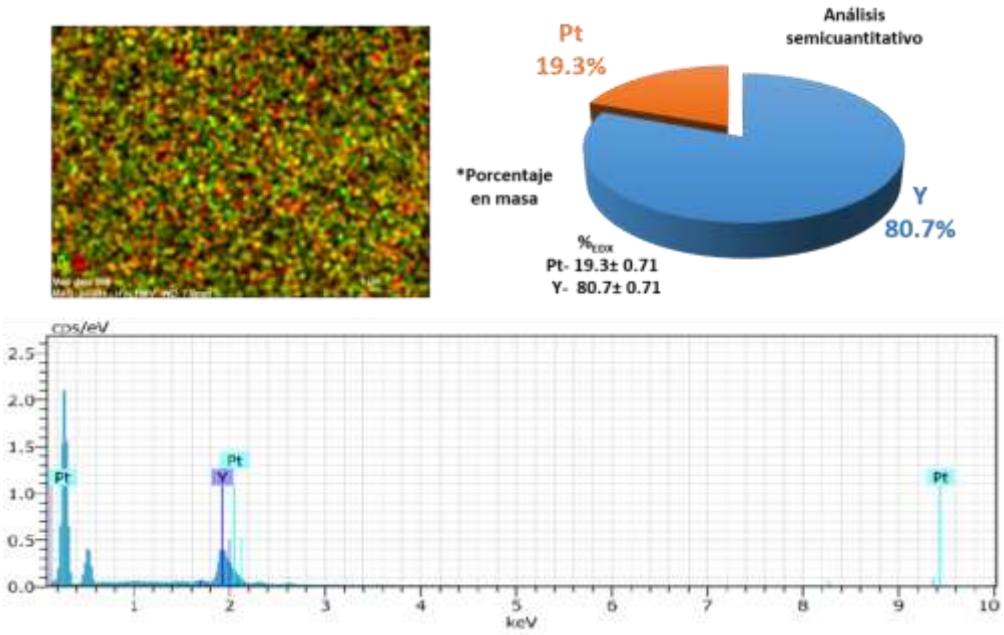

Fig. 3 Images of the elemental phase distribution of Y and Pt obtained by EDX mapping

Fig. 4B, shows the corresponding CO_{ad} stripping curves, after second scan subtraction previously cycled

30 times between 0.5 V and 1.2 V. CO electro-oxidation was used to determine the specific surface area from the normalized curves, considering the charge takes to oxidized the pre-adsorbed monolayer of CO, The charge of full coverage for clean polycrystalline Pt is Q_{CO}= 420 μC cm^{-2} and is used as the conversion

factor. The Pt electrochemical surface area ($ECSA_{Pt,cat}$) is reported in $m^2\ g_{Pt}^{-1}$; L_{Pt} is the working electrode Pt loading ($mg_{Pt}\ cm^{-2}$) and A_g (cm^2) is the geometric surface area of the glassy carbon electrode (i.e., 0.196 cm^2). According to the equation (2) given the ECSA for Y@Pt of 66.41 $m^2\ g_{Pt}^{-1}$, higher than reported for platinum [11]

$$ECSA_{Pt,Cat}\ (m^2 g_{Pt}^{-1}) = \left[\frac{Q_{CO}\ (C)}{420\mu C cm^{-2} L_{Pt}(mg_{Pt}\,cm^{-2}) A_g(cm^2)}\right] 10^5 \quad (2)$$

After CV characterization, the catalysts were evaluated using RDE technique for assessing their electrocatalytic activity and stability for ORR. The Fig. 5A shows a typical set of polarization curves for the ORR on Y@Pt. By starting at 1.05 V and scanning the electrode potential negatively, a mixed kinetic-diffusion control region between $0.85 \leq E \geq 0.95$ V is followed by a defined diffusion-limiting current bellow 0.85 V. The Y@Pt sample showed half-wave potential of $\Delta E_{1/2} = 0.90$ V with a small positive shift compared with platinum $\Delta E_{1/2} = 0.89$ V [11]. In addition to be close to values previously reported in Y-Pt alloys [12][13][14].

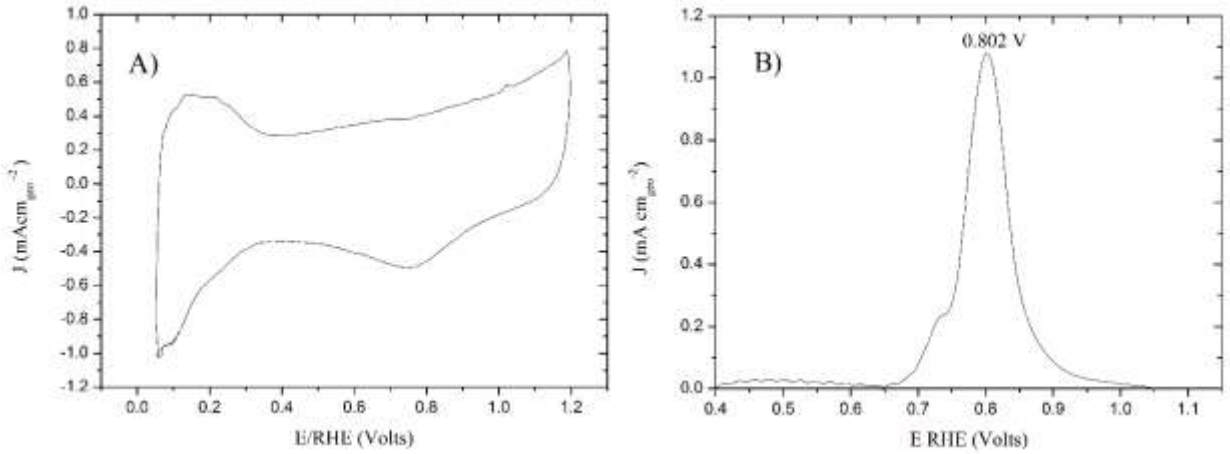

Fig. 4 (A) Base voltammograms on N_2-purged (B) CO_{ad} stripping voltammograms on Y@Pt nanoparticles. The voltammograms were carried out in 0.1 M $HClO_4$ at room temperature and scan rate of 20 mV s^{-1}.

The Fig. 5B, shows the Tafel plots for the mass transport corrected surface specific current density, obtained from the negative sweep direction at 1600 rpm using Eq (3) in potentials between $0.85 \leq E \geq 0.95$ V.

$$J_k = \frac{J_L J}{J_L - J} \quad (3)$$

Tafel slope is shifted positively with respect to Pt (not shown), showing a noticeably activity increase.

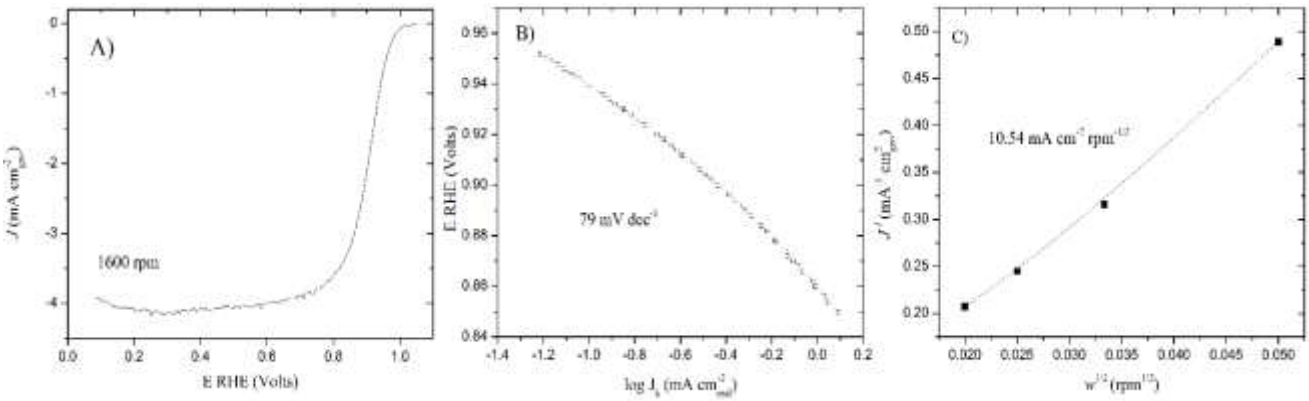

Fig. 5 (A) Steady-state polarization curves for the ORR, and (B) mass-transfer corrected Tafel plot (C) Kouteckye-Levich plots in O_2 saturated 0.1 M $HClO_4$.

Fig. 5C shows the inverse of the overall limiting current density (J^{-1}), as a function of the inverse square root of the rotation rate ($w^{-1/2}$), known as Kouteckye-Levich plot Ec (4).

$$\frac{1}{J} = \frac{1}{J_k} + \frac{1}{J_L} + \frac{1}{J_f} = \frac{1}{J_k} + \frac{1}{Bw^{1/2}} \qquad (4)$$

The linear relation between J^{-1} vs $w^{-1/2}$, in the plot indicated a first order kinetic and in agreement with the theoretical slope value, i.e. $B_0 = 12.63 \times 10^{-2}$ mA cm^{-2} rpm$^{-1/2}$, calculated considering a four-electron transfer process leading to water formation, i.e., $O_2 + 4H^+ + 4e^- \rightarrow 2H_2O$.

The most relevant results are summarized in Table 1.

Table 1. Values of kinetic parameters for the ORR on Pt and Y@Pt at 20 mV^{s-1}.

Electrode	$E_{1/2}$ (mV)	ECSA $m^2\ g_{Pt}$	$B_0 \times 10^{-2}$ (mA/cm^2 rpm$^{1/2}$)	Tafel slope (mV/dec)[a]	$J_{k0.9}$ (mA/cm$^2_{Pt}$)	$J_{m0.9}$ (mA/mg$_{Pt}$)
Pt	0.89 [c]	61	13.7 [b]	88.7[b]	0.347 [c]	210 [c]
Y@Pt [d]	0.90	66	10.54	78.6	0.365	229

[a] Tafel slope were obtained between 0.9 - 0.8V for Pt and .95-.85V for Y@Pt. [b] Data taken from [15] in 0.5 M H_2SO_4 [c] Data taken from [11] [d] Datas in 0.1 $HClO_4$.

4. Summary and perspectives

Well defined carbon supported Y@Pt core-shell nanocatalysts with around 2 nm size were synthesized through chemical reduction and galvanic replacement.

X-ray diffraction for the catalyst sample showed phases of Pt3Y, Pt and Carbon with composition relative of two phases assigned to metallic Pt and C in the relative weight fraction of 2.3 wt% and 97.3 wt. %, respectively. The change in the reflection profile suggests a strong interaction between Pt and Y which resulted in a Pt lattice contraction and a possible lattice expansion for Y. The CV in the O_2 free electrolyte resembled that of pure Pt and confirms a complete Pt shell covering Y-core. The Y@Pt shows an ECSA of 66 m^2 g_{Pt}. The RRDE measurement shows a catalytic activity enhancement with respect to pure platinum.

Acknowledgements

This work was supported by CONACYT (grant FOINS/75/2012). The authors gratefully acknowledge to University of Texas TAMU for the TAMU-CONACYT project (Alloy nanocatalysts for fuel cell electrodes). The authors gratefully acknowledge also to Josue E. Romero Ibarra and Daniel Bahena Uribe for the support in the SEM and TEM. Techniques and José Luis Reyes-Rodríguez for their support in the development of this work.

References

[1] C.W.B. Bezerra, L. Zhang, K. Lee, H. Liu, A.L.B. Marques, E.P.Marques, H. Wang and J. Zhang, A review of Fe–N/C and Co–N/C catalysts for the oxygen reduction reaction. Electrochimica Acta 2008; 53:4937-4951.

[2] P.H. Matter, L. Zhang and U.S. Ozkan, The role of nanostructure in nitrogen-containing carbon catalysts for the oxygen reduction reaction. Journal of Catalysis 2006; 239: 83-96.

[3] V. Mazumder, M. Chi, K.L. More and S. Sun. Core/Shell Pd/FePt Nanoparticles as an Active and Durable Catalyst for the Oxygen Reduction Reaction. J. Am. Chem. Soc. 2010; 132:7848-7849.

[4] V.R. Stamenkovic , B. Fowler, B.S. Mun, G. Wang, P.N. Ross, C.A. Lucas, N.M. Markovic, Improved oxygen reduction activity on Pt3Ni(111) via increased surface site availability. Science 2007; 315:493-497.

[5] J.K. Nørskov, J.Rossmeisl, A. Logadottir, L. Lindqvist, J.R. Kitchin, T. Bligaard, et al. Origin of the overpotential for oxygen reduction at a fuel-cell cathode. J. Phys Chem B 2004; 108: 17886-17892.

[6] J. Zhang, M.B. Vukmirovic, K. Sasaki, A.U. Nilekar , M. Mavrikakis and R.R. Adzic, Mixed-metal Pt monolayer electrocatalysts forenhanced oxygen reduction kinetics. J Am Chem Soc 2005; 127:12480-12481.

[7] V.R. Stamenkovic, B.S. Mun , M. Arenz, K.J.J. Mayrhofer, C.A. Lucas, G. Wang, et al. Trends in electrocatalysis on extended and nanoscale Pt-bimetallic alloy surfaces. Nat Mater 2007; 6:

241-247.

[8] J.L. Reyes-Rodríguez, F. Godínez-Salom+on, M.A. Leyva and O. Solorza-Feria, RRDE study on Co@Pt/C coreeshell nanocatalysts for the oxygen reduction reaction, International journal of hydrogen energy 2013; 38: 12634-12639.

[9] J.X. Wang, H. Inada, L. Wu, Y. Zhu, Y. Choi, P. Liu, W.P. Zhou and R.R. Adzic,Oxygen Reduction on Well-Defined Core-Shell Nanocatalysts: Particle Size, Facet, and Pt Shell Thickness Effects, J. Am. Chem. Soc. 2009; 131: 17298-17302.

[10] J. Maruyama, I. Abe, Influence of anodic oxidation of glassy carbon surface on voltammetric behavior of Nafion®-coated glassy carbon electrodes, Electrochimica Acta 2001;46: 3381–3386.

[11] Y. Garsany, O.A. Baturina, K. E. Swinder-Lyons and S.S. Kocha Experimental Methods for Quantifying the Activity of Platinum Electrocatalysts for the OxygenReduction Reaction Anal. Chem. 2010; 82: 6321–6328.

[12] S.J. Yoo, K.S. Lee, S.J. Hwang, Y.H Cho, S.K. Kim, J.W. Yun, Y.E. Sung and T.H. Lim Pt3Y electrocatalyst for oxygen reduction reaction in proton exchange membrane fuel cells, International journal of hydrogen energy 2012; 37: 9758-9765.

[13] S.J. Hwang, S.K. Kim, J.G. Lee, S.C. Lee, J.H. Jang, P. Kim, et. al. Role of Electronic Perturbation in Stability and Activity of Pt-Based Alloy Nanocatalysts for Oxygen Reduction, Journal of the American Chemical Society 2012; 134:19508-19511.

[14] J. Greely, I.E.L. Stephens, A.S. Bondarenko, T.P. Johansson, H.A. Hansen, T.F, Jaramillo, J. Rossmeisl, I. Chorkendorff and J.K. Norskov Alloys of platinum and early transition metals as oxygen reduction electrocatalysts Nature Chemistry; 1:552-556.

[15] F.Godínez-Salomón, M.Hallen-López and O. Solorza-Feria,Enhanced electroactivity for the oxygen reduction on Ni@Pt core-shell nanocatalysts, International journal of hydrogen energy 2012; 37: 14902-14910.